Unconventional Ribbon-Shaped β-Ga_2O_3 Tubes with Mobile Sn Nanowire Fillings

Junqing Hu,[†,‡,*] Quan Li,[§,*] Jinhua Zhan,[⊥] Yang Jiao,[§] Zongwen Liu,[#] Simon P. Ringer,[#] Yoshio Bando,[†,⊥] and Dmitri Golberg[⊥]

[†]International Center for Young Scientists, National Institute for Materials Science, Namiki 1-1, Tsukuba, Ibaraki 305-0044, Japan, [‡]College of Materials Science and Engineering, State Key Laboratory for Modification of Chemical Fibers and Polymer Materials, Donghua University, Shanghai 200051, China, [§]Department of Physics, The Chinese University of Hong Kong, Shatin, New Territory, Hong Kong, [⊥]Nanoscale Materials Center, National Institute for Materials Science, Namiki 1-1, Tsukuba, Ibaraki 305-0044, Japan, and [#]Australian Key Centre for Microscopy and Microanalysis, University of Sydney, Sydnes, NSW 2006, Australia

ABSTRACT We report on the synthesis of novel, unconventional β-Ga_2O_3 tubes *via* a Sn nanowire template process using thermal decomposition and oxidation of SnO and GaN powder mixtures. Distinctly different from any previously reported nano- and microtubes, the present β-Ga_2O_3 tubes display a flattened and thin belt-like (or ribbon-like) morphology. Each ribbon-shaped tube has a width of ~1–2 μm over its entire length, a length in the range of tens of micrometers, a thickness of ~100–150 nm, and a uniform inner diameter of 30–120 nm. The tubes were either partially or completely filled with Sn nanowires, forming Sn/Ga_2O_3 metal−semiconductor nanowire heterostructures. A convergent electron beam generated in a transmission electron microscope is demonstrated to be an effective tool for delicate manipulation of encapsulated Sn nanowires. The Sn nanowires were gently cut apart (into two discrete fragments) and then completely separated and rejoined within Ga_2O_3 ribbon-shaped tubes. These unconventional β-Ga_2O_3 tubes not only should enrich the well-established bank of nanostructured morphologies and extend the understanding of crystal growth at the nanoscale but also may have promise for the design of electron-beam-irradiation- or thermo-driven electrical switches.

KEYWORDS: ribbon-shaped tubes · β-Ga_2O_3 · Sn nanowire · electron beam irradiation · electrical switches

Monoclinic gallium oxide (β-Ga_2O_3), one of the transparent conducting oxides, is an insulator with a wide band gap of ~4.9 eV and becomes an n-type semiconductor when synthesized under reducing conditions.[1,2] β-Ga_2O_3 is useful as insulating oxide layer for all gallium-based semiconductors and can also be applied as an optical limiter for ultraviolet light and as an oxygen gas sensor.[3] Because of the novel properties of carbon nanotubes, one-dimensional nanostructures, such as wires, tubes, and ribbons, have attracted extensive interest over the past decade. Such structures have a great potential for addressing some basic issues related to dimensionality and space-confined transport phenomena, and for practical applications.[4] So far, there has been great progress in the development of new nanotubes based on metal oxides (including β-Ga_2O_3),[5–8] sulfides,[5–12] nitrides,[13,14] elemental species,[15,16] and others.[17–20] These tubular structures have a common characteristic related to a hollow morphology and may possess a circular, square-like, or hexagon-like cross section. Herein, we report a distinctly different tubular structure of β-Ga_2O_3 that has a flattened and thin belt-like (or ribbon-like) morphology with a circular inner channel. Such nonstandard tubes were either partially or completely filled with Sn nanowires, thus forming Sn/Ga_2O_3 metal−semiconductor nanowire heterostructures. A convergent electron beam (EB) generated in a transmission electron microscope (TEM) is demonstrated to be an effective tool for delicate manipulation of a Sn nanowire; *i.e.*, it can be gently cut apart into two segments, which

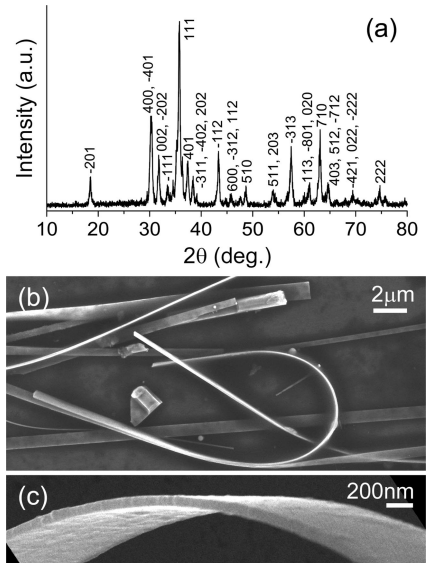

Figure 1. (a) XRD pattern and (b,c) SEM images of the β-Ga_2O_3 ribbons.

*Address correspondence to HU.Junqing@nims.go.jp, liquan@sun1.phy.cuhk.edu.hk.

Received for review October 8, 2007 and accepted December 06, 2007.

Published online December 22, 2007. 10.1021/nn700285d CCC: $40.75

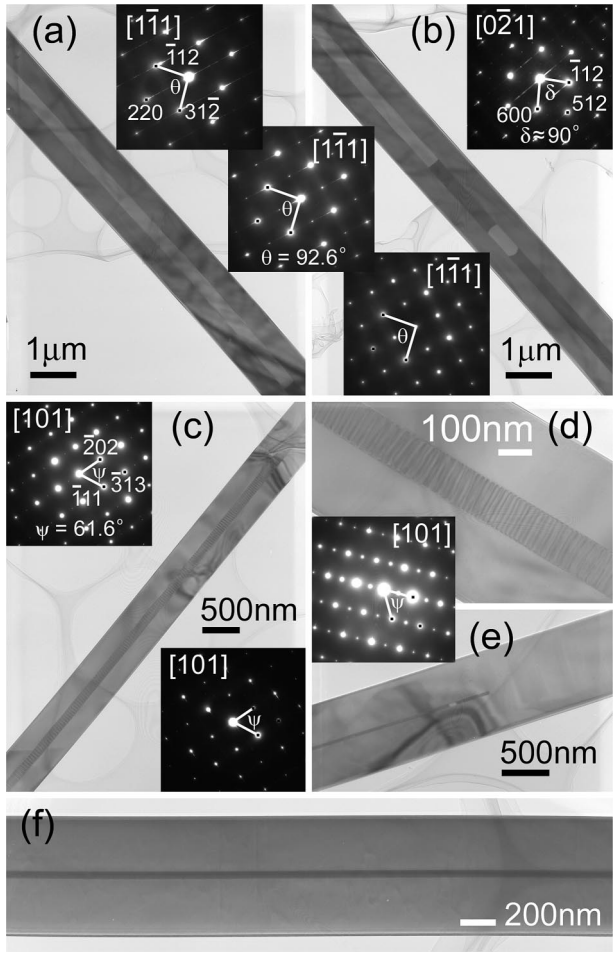

Figure 2. TEM images of the β-Ga_2O_3 RSTs. (a) A hollow tube and the corresponding ED patterns recorded from tube's edge domains (upper and middle insets) and center (lower inset), respectively, all of which are indexed to the [1–11] zone axis patterns of β-Ga_2O_3. (b) A tube partially filled with a Sn nanowire and the corresponding ED pattern, which is indexed to the [0–21] zone axis pattern of β-Ga_2O_3. (c) A tube completely filled a Sn nanowire, forming a Sn/Ga_2O_3 metal−semiconductor nanowire heterostructure, and the corresponding ED patterns recorded from the tube edge and the Sn-filled domain, both of which can be indexed to the [101] zone axis patterns of β-Ga_2O_3. (d) A high-magnification TEM image of the structure shown in panel c. (e,f) Small inner diameter β-Ga_2O_3 tubes (*i.e.*, fine-diameter Sn nanowire fillings) and the corresponding ED pattern, which can be indexed to the [101] zone axis pattern of β-Ga_2O_3.

can be spatially separated and rejoined together through electron-beam-induced melting and a beam-driven move inside a Ga_2O_3 tube. The findings on the present flattened ribbon-shaped tubes (RSTs) not only widen the pre-existing range of existing nanostructures and extend the understanding of crystal growth at the nanoscale but may also stimulate a practical design of new functional electron-beam-irradiation- or thermo-driven electrical switches.

RESULTS AND DISCUSSION

After the synthesis, a white wool-like product was obtained from the silicon wafers inside the tube furnace. An X-ray diffraction (XRD) pattern of the product is shown in Figure 1a. All the diffraction peaks can be indexed to those of a monoclinic structure of β-Ga_2O_3 (JCPDS 43-1012; *C*2/*m*, $a = 12.23$ Å, $b = 3.04$ Å, $c = 5.80$ Å, and $\beta = 103.7°$). The scanning electron microscopy (SEM) image in Figure 1b reveals the general morphology of the product. Long and straight ribbons are observed. The yield of the β-Ga_2O_3 ribbons in the synthesized product was estimated to be 30–40%, based on the amount of the starting GaN powder used. Each ribbon has a uniform width of ~1–2 μm over its entire length, and a length in the range of tens of micrometers. The high-magnification SEM image in Figure 1c further suggests uniform ribbon-shaped geometrical characteristics. The ribbon thickness can be deduced from its edge-on image and is estimated to be ~100–150 nm. The typical width-to-thickness ratio of the β-Ga_2O_3 ribbons was ~5−10.

The microstructure and chemical composition of the product were investigated in detail by transmission electron microscopy (TEM). As can be clearly seen from the TEM images in Figure 2, each β-Ga_2O_3 ribbon is actually not a monolithic "ribbon" but has a central hollow or Sn nanowire-filled channel. Further analysis of the RSTs using energy-dispersive X-ray (EDX) analysis verified their chemical compositions, as will be discussed later. The unconventional RSTs all have very thin and uniform inner channels of ~30–120 nm diameter. Figure 2a shows a hollow tube, for which electron diffraction patterns (DPs) are taken from its edge domains (upper and middle insets, Figure 2a) and its center (lower inset, Figure 2a,b), respectively. By checking the characteristic angles and spacings on the DPs, the most intense reflections are assigned to the [1–11] zone axis of β-Ga_2O_3. However, some extra reflections (middle and lower insets) are also clearly observed at the extinctive positions of the [1–11] zone axis DP of β-Ga_2O_3 and are due to a symmetry corresponding to the space group *C*2/*m* (a reflection condition is $h + k = 2n$). Those weaker reflections are identified to be high-order Laue reflections, which are also frequently observed in standard β-Ga_2O_3 nanoribbons.[21] The appearance of the high-order Laue zone reflections is due to the fact that the β-Ga_2O_3 RSTs are very thin. Figure 2b shows discrete Sn nanowire segments filling a β-Ga_2O_3 tube, thus forming separate hollow domains. The upper-right inset shows corresponding DPs taken from either hollow or Sn nanowire-filled parts, which can be indexed to the [0–21] zone axis of β-Ga_2O_3. Figure 2c depicts a completely filled tube, *i.e.*, a Sn/Ga_2O_3 metal−semiconductor nanowire heterostructure. The upper-left and lower-right insets show the ED patterns recorded from the tube edge and a filled domain, both of which can be indexed to the [101] zone axis of β-Ga_2O_3. Some very weak reflections seen in the upper inset pattern are also due to high-order Laue reflections. Interestingly enough, in these ED patterns, no diffraction spots originating from crystalline Sn nanowires are visible. This

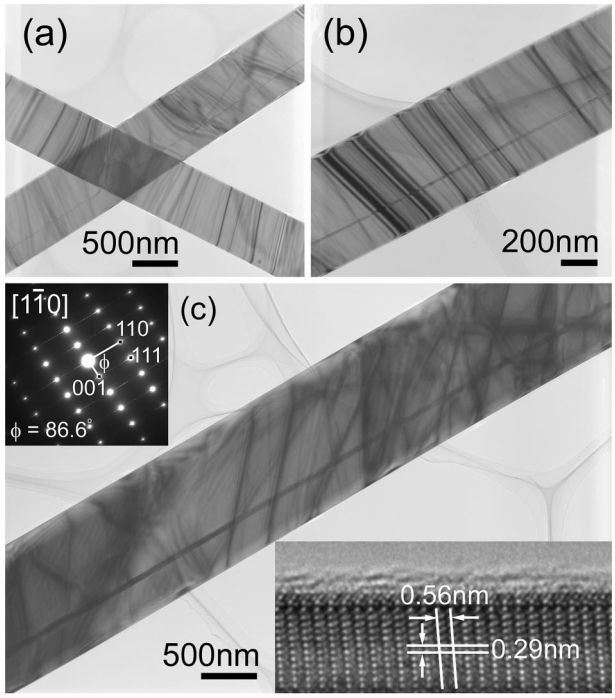

Figure 3. TEM images of β-Ga_2O_3 RSTs, in which the long symmetry axis of the tube cavities (or the Sn nanowire fillings) diverges from the long symmetry axis of the ribbon matrix (or tube walls), and the corresponding ED pattern (upper-left inset in panel c), which can be indexed to the [1–10] crystal zone of β-Ga_2O_3, and HRTEM image (lower-right inset).

implies that, during the present TEM imaging, they were in a liquid state (as will be discussed later). The contrast variations on the ribbons along the embedded Sn nanowire axes suggest that many steps exist on the inner wall of the β-Ga_2O_3 nanostructure, as shown in the high-magnification TEM image in Figure 2d. In some structures, the inner diameters of the channels and thus Sn nanowire fillings are as small as ~10–20 nm (Figure 2e,f), quite different from the micrometer-scale dimensions of the whole nanostructures. In a few of the structures, the tubular narrow cavity does not span the ribbon's whole length (Figure 2e), but instead it terminates inside a ribbon. The ED pattern in the upper-left inset is the same as that shown in Figure 2c. It again can be indexed to the [101] zone axis of β-Ga_2O_3. Similarly, due to high-order Laue reflections, some extra intense reflections appear in this pattern, suggesting a very thin β-Ga_2O_3 RST.

In a standard tubular structure, a cavity is located at the center and extends over the entire length, so that the tube cavity and the tube wall have the same symmetry axis. Structures in which the internal cavity strongly deviates from the center of symmetry toward one side are rather rare. Here, we observed rarely seen β-Ga_2O_3 tubes, as shown in Figure 3a–c. In these β-Ga_2O_3 tubes, a channel is notably shifted out of the nanostructure's center of symmetry. This may represent a new, interesting growth phenomenon for tubular crystal structures. Many streak-like or ripple-type contrasts are observed over the thin tubular ribbons (Figure 3). This is a common diffraction phenomenon most frequently observed in thin TEM samples due to deformation and bending.[22] The ED pattern shown in the inset in the upper left of Figure 3c can be indexed to the [1–10] zone axis of β-Ga_2O_3. The inset in the lower right in this figure shows a high-resolution TEM image taken from this novel tube, which implies its perfect crystallinity: the measured *d*-spacings of 0.56 and 0.29 nm are in accordance with the {001} and {110} crystallographic planes of β-Ga_2O_3, respectively. The long-axis direction, or the growth direction of the tube, is nearly parallel to the [001] crystallographic orientation of β-Ga_2O_3.

Figure 4a is a scanning transmission electron microscopy (STEM) image of a Sn nanowire-filled β-Ga_2O_3 RST. The respective Ga, O, and Sn elemental maps are shown in Figure 4b–d. They demonstrate the well-defined composition variations and a clear interface between a Sn nanowire filling and a β-Ga_2O_3 ribbon matrix. EDX spectra generated with an electron nanoprobe (~20 nm in diameter) were collected from the Sn nanowire filling and β-Ga_2O_3 ribbon matrix, respectively. They confirmed the chemical compositions of Sn and Ga_2O_3 within this Ga_2O_3 RST.

During our experiments, a convergent 300 kV EB generated in a field emission TEM was found to be

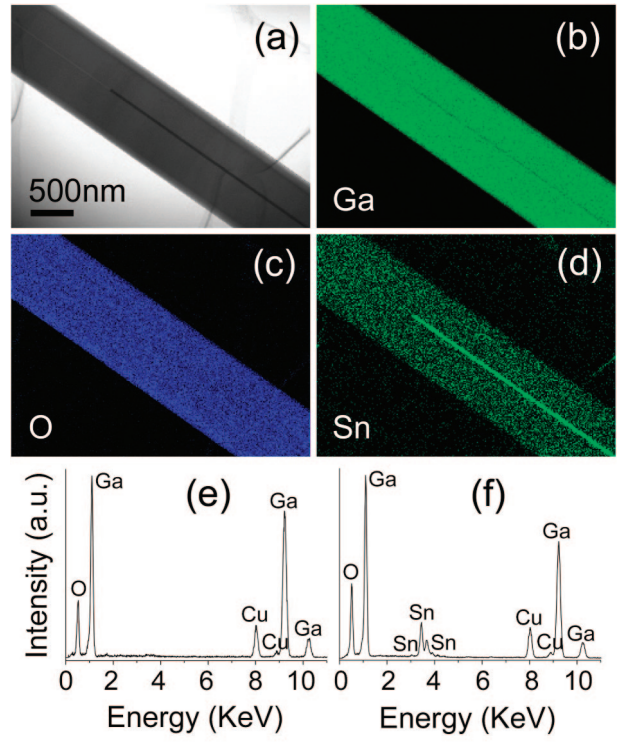

Figure 4. (a) STEM image of a Sn nanowire-filled β-Ga_2O_3 RST, along with (b) Ga, (c) O, and (d) Sn elemental maps. (e,f) EDX spectra taken from the Ga_2O_3 ribbon matrix and Sn nanowire filling, respectively.

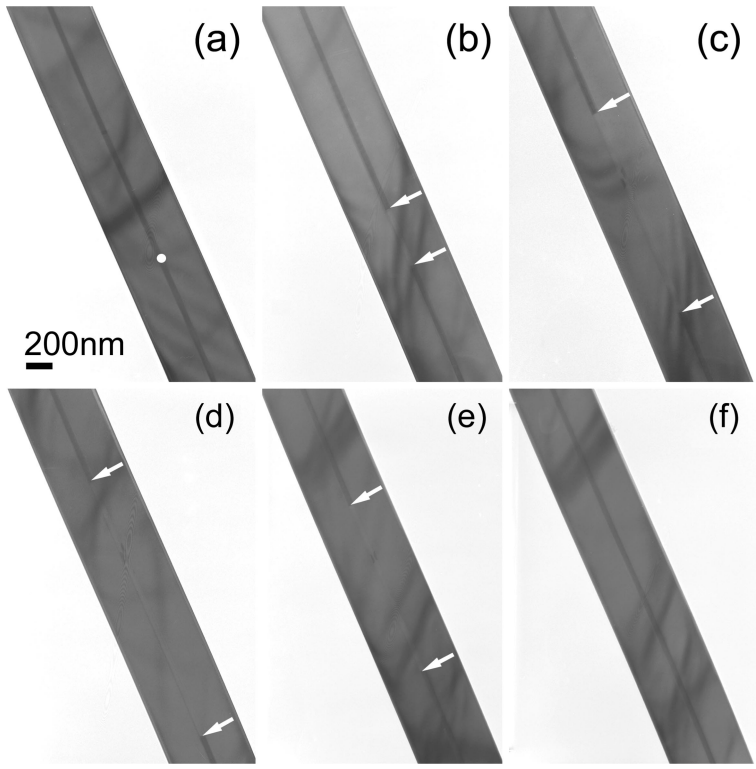

Figure 5. Consecutive TEM images displaying a process of cutting apart (a,b), removing (c,d), and rejoining (e,f) the Sn nanowires inside a β-Ga_2O_3 RST under convergent EB irradiation.

an effective tool for manipulation of the Sn nanowires: they may be gently cut apart (into two discrete nanowires), separated, and rejoined within a Ga_2O_3 RST. For example, the beam was focused on a Sn nanowire filling within a spot ~30 nm in diameter, as marked by the white dot on the initial TEM image in Figure 5a. After this intense irradiation over 3 min, the filled Sn nanowire was melted and then cut into two discrete Sn nanowires. After an additional ~2 min of irradiation on the region, the two Sn fragments separated from each other, forming a gap of ~500 nm between them (Figure 5b). The focused beam diameter was then increased to ~100 nm. It was moved up (to ~600 nm) to the top of the upper Sn domain and then down to its bottom (along the Sn nanowire axis); after tens of cycles, the Sn nanowire segment expanded upward due to beam-induced heating. Through a similar EB manipulation with the bottom Sn nanowire, this segment can be continuously shifted downward, so that the separation gap between the two segments extends to ~1700 nm (Figure 5c) and ~2100 nm (Figure 5d). Interestingly, when the beam was kept away from but very close to the Ga_2O_3 ribbon matrix, the Sn nanowire fragments moved in opposite directions while the gap shrank to ~1300 nm (Figure 5e). When the beam was gradually moved away from the specimen, the two Sn nanowires further approached each other and finally merged into a single filling; thus, the original nanowire shape inside the Ga_2O_3 tube is entirely recovered.

It is known that the melting point of nanostructured materials can be much lower than that of their bulky counterparts (for example, the difference between the melting point of Au nanoparticles and Au bulk material is over 400 °C[23,24]). So, it is reasonable to assume that there is a significant difference between the melting point of the present tiny Sn nanowires and a Sn bulk material (bulk Sn, mp = 232 °C[25]). On the other hand, when an EB passes through a specimen, its energy will be partially transferred to thermal energy *via* inelastic scattering processes and thus may result in a significant local temperature rise and/or change in the material crystal structures.[26,27] In the present case, under electron irradiation, the temperature in the vicinity of the Sn nanowire increases. Consequently, a Sn nanowire may entirely melt (even though the melting point of bulk metallic Sn is far above room temperature) and then thermally expand at a very low basic pressure (~1×10^{-5} Pa) in the TEM chamber. This drives the Sn nanowires within a Ga_2O_3 RST. When the beam is gradually moved out of the Sn nanowire area, the Sn nanowires cool down and merge inside the tube. This sequence of events indicates that a convergent EB is an effective tool for nanoscale manipulation with a Sn liquid nanowire within Ga_2O_3 RSTs. The controlled thermal expansion and movement of a Sn nanowire inside a Ga_2O_3 RST can make the design of EB- and temperature-driven electrical switches and/or sensors possible.

For the growth of the Sn nanowire-filled Ga_2O_3 RSTs, thermal decomposition of SnO and oxidation of GaN powders at a high temperature may be combined. As depicted in Figure 6a, a possible model for the growth of Sn nanowire-filled Ga_2O_3 RSTs is postulated as follows. It is known that SnO should decompose to Sn and SnO_2 above 300 °C.[25] The higher the reaction temperature, the faster is the decomposition rate.[28,29] Sn (bp = 2270 °C[25]) is in the form of small liquid clusters when reduced from SnO. The Sn clusters are then

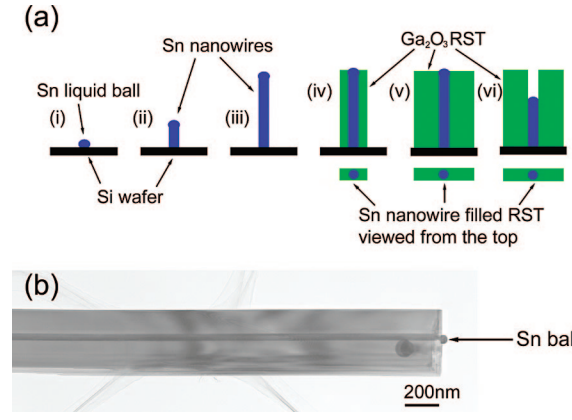

Figure 6. Schematic depicting a possible growth model for the Sn nanowire-filled Ga_2O_3 RSTs.

transported by a carrier gas to a lower temperature region, where they deposit in the form of liquid nanoscale balls on the silicon wafers inside the alumina tube (step i). As-formed Sn balls readily absorb a Sn flux, thus initiating the one-dimensional growth of Sn nanowires *via* a traditional vapor–liquid–solid (VLS) process (steps ii and iii). The liquid Sn ball, inherent to the VLS mechanism, was found on the tip of the Sn nanowire (Figure 6b). This fact also suggests that the VLS mechanism was due to the growth of the Sn nanowires. In the present VLS growth of Sn nanowires, no additional transition metals are added as catalysts; it is, therefore, believed that the formation of the Sn nanowires undergoes a self-catalyzed VLS growth process. The newly formed Sn functions as a nanowire seed, which further grows to a Sn nanowire in the presence of Sn vapor. (The self-catalyzed VLS growth process has been systematically demonstrated in our previous reports.[30–32]) As the reaction temperature reaches 1200 °C, the GaN powders should also decompose into dense Ga small clusters and N_2. Due to the insurmountable presence of a small amount of oxygen within the system,[33] there may exist gallium oxide clusters in the reaction chamber. As-formed gallium oxide clusters are also transferred downstream by the carrier gas to a position where the Sn nanowire has been growing, and then the Ga_2O_3 clusters are deposited on the Sn nanowire surface. It is reasonable to suggest that the Sn nanowires serve as templates for the deposition of Ga_2O_3 clusters. In the present thermodynamic conditions, newly arriving Ga_2O_3 clusters may deposit on the formed Ga_2O_3 nucleus while the surfaces that have a lower energy start to form, such as the side surfaces (step iv).[34,35] As long as the Ga_2O_3 clusters are available, the low-energy side surfaces' growth tends to be flat (step v). This prevents the accumulation of incoming Ga_2O_3 clusters on the surfaces, finally resulting in the formation of a Ga_2O_3 ribbon containing a Sn nanowire, *i.e.*, a Sn nanowire-filled Ga_2O_3 RST. Long-time annealing would lead to thermal expansion of Sn nanowires within the tube channels or their partial removal from the tubes. As a result, Ga_2O_3 RSTs with partial Sn nanowire fillings and partially hollow cavities form (step vi).

CONCLUSIONS

Novel unconventional β-Ga_2O_3 tubes were synthesized *via* a Sn nanowire template process through thermal decomposition and oxidation of a mixture of SnO and GaN powders. Distinctly different from any previously reported nano- and microtubes, the present β-Ga_2O_3 tubes display flattened and thin belt-like (or ribbon-like) morphologies, which are not common for any known tubular structures. The tubes were either partially or completely filled with Sn nanowires, thus forming Sn/Ga_2O_3 metal−semiconductor nanowire heterostructures. A convergent electron bean generated in a transmission electron microscope was demonstrated to be an effective tool for delicate manipulation with a given Sn nanowire: the nanowire can be gently cut apart (into discrete fragments), and the parts may then be separated and rejoined within a Ga_2O_3 ribbon-shaped tube. We envisage that the present β-Ga_2O_3 tubes would not only enrich the well-established spectrum of the tubular structures and extend the understanding of crystal growth at the nanoscale but also promote the design of functional electron-beam-irradiation- or thermo-driven electrical switches.

METHODS

The flattened ribbon-shaped, Sn nanowire-filled Ga_2O_3 tubes were grown using a high-temperature vacuum tube furnace, the setup of which was described elsewhere.[36,37] Briefly, a mixture of GaN and SnO was placed on an alumina boat in the central region of an alumina tube. Several strip-like Si wafers, ultrasonically cleaned in acetone, were used as substrates and placed on a wide alumina plate, which was inserted downstream into the tube. The tube was then pumped down to a base pressure of 2×10^{-2} Torr. A constant flow of Ar mixed with 10% H_2 was introduced into the tube at a flow rate of 150 sccm. The furnace was heated at a rate of 30 °C/min to 900 °C and maintained at that temperature for 1 h, followed by further heating to and holding at 1200 °C for 2 h before it was finally cooled to room temperature. The total pressure was maintained at 350 Torr during the fabrication process. The products collected from the Si wafers were characterized using X-ray powder diffraction (RINT 2200) with Cu Kα radiation, scanning electron microscopy (S-4800), and transmission electron microscopy (JEM-3000F and JEM-2100F equipped with an energy-dispersive X-ray spectrometer).

Acknowledgment. This work was performed through the Special Coordination Funds for Promoting Science and Technology from the Ministry of Education, Culture, Sport, Science, and Technology of the Japanese Government (Japan), Program for Specially Appointed Professor by Donghua University (China), and the RGC grant of the HKSAR under project no. 413706 (Hong Kong SAR). The authors thank Prof. X. M. Meng of the Lab of Optoelectronic Functional Materials and Molecular Engineering, Technical Institute of Physics and Chemistry, Chinese Academy of Science, Beijing 100080, P. R. China, for helpful discussions about TEM images.

REFERENCES AND NOTES

1. Binet, L.; Gourier, D. Origin of the Blue Luminescence of Beta-Ga_2O_3. *J. Phys. Chem. Solids* **1998**, *59*, 1241–1249.
2. Li, J. Y.; Qiao, Z. Y.; Chen, X. L.; Chen, L.; Cao, Y. G.; He, M.; LI, H.; Cao, Z. M.; Zhang, Z. Synthesis of Beta-Ga_2O_3 Nanorods. *J. Alloys Compd.* **2000**, *306*, 300–302.
3. Choi, Y. C.; Kim, W. S.; Park, Y. S.; Lee, S. M.; Bae, D. J.; Lee, Y. H.; Park, G.-S.; Choi, W. B.; Lee, N. S.; Kim, J. M. Catalytic Growth of Beta-Ga_2O_3 Nanowires by Arc Discharge. *Adv. Mater.* **2000**, *12*, 746–750.
4. Dekker, C. Carbon Nanotubes as Molecular Quantum Wires. *Phys. Today* **1999**, *52*, 22–28.
5. Hoyer, P. Formation of a Titanium Dioxide Nanotube Array. *Langmuir* **1996**, *12*, 1411–1413.
6. Cheng, B.; Samulski, E. T. Fabrication and Characterization of Nanotubular Semiconductor Oxides In_2O_3 and Ga_2O_3. *J. Mater. Chem.* **2001**, *11*, 2901–2902.

7. Sharma, S.; Sunkara, M. K. Direct Synthesis of Gallium Oxide Tubes, Nanowires, and Nanopaintbrushes. *J. Am. Chem. Soc.* **2002**, *124*, 12288–12293.
8. Hu, J. Q.; Li, Q.; Meng, X. M.; Lee, C. S.; Lee, S. T. Thermal Reduction Route to the Fabrication of Coaxial Zn/ZnO Nanocables and ZnO Nanotubes. *Chem. Mater.* **2003**, *15*, 305–308.
9. Tenne, R.; Margulis, L.; Genut, M.; Hodes, G. Polyhedral and Cylindrical Structures of Tungsten Disulfide. *Nature* **1992**, *360*, 444–446.
10. Tenne, R.; Homyonfer, M.; Feldman, Y. Nanoparticles of Layered Compounds with Hollow Cage Structures (Inorganic Fullerene-Like Structures). *Chem. Mater.* **1998**, *10*, 3225–3238.
11. Nath, M.; Govindaraj, A.; Rao, C. N. R. Simple Synthesis of MoS_2 and WS_2 Nanotubes. *Adv. Mater.* **2001**, *13*, 283–286.
12. Hu, J. Q.; Bando, Y.; Zhan, J. H.; Liu, Z. W.; Golberg, D. Uniform and High-Quality Submicrometer Tubes of GaS Layered Crystals. *Appl. Phys. Lett.* **2005**, *87*, 153112.
13. Goldberger, J.; He, R. R.; Zhang, Y. F.; Lee, S.-K.; Yan, H. Q.; Choi, H.-J.; Yang, P. D. Single-Crystal Gallium Nitride Nanotubes. *Nature* **2003**, *422*, 599–602.
14. Hu, J. Q.; Bando, Y.; Golberg, D.; Liu, Q. L. Gallium Nitride Nanotubes by the Conversion of Gallium Oxide Nanotubes. *Angew. Chem., Int. Ed.* **2003**, *42*, 3493–3497.
15. Hu, J. Q.; Bando, Y.; Liu, Z. W.; Zhan, J. H.; Golberg, D.; Sekiguchi, T. Synthesis of Crystalline Silicon Tubular Nanostructures With ZnS Nanowires as Removable. *Angew. Chem., Int. Ed.* **2004**, *43*, 63–66.
16. Mo, M. S.; Zeng, J. H.; Liu, X. M.; Yu, W. C.; Zhang, S. Y.; Qian, Y. T. Controlled Hydrothermal Synthesis of Thin Single-Crystal Tellurium Nanobelts and Nanotubes. *Adv. Mater.* **2002**, *14*, 1658–1662.
17. Martin, C. R. Nanomaterials—Membrane-Based Synthetic Approach. *Science* **1994**, *266*, 1961–1966.
18. Ajayan, P. M.; Stephan, O.; Redlich, P.; Colliex, C. Carbon Nanotubes as Removable Templates for Metal-Oxide Nanocomposites and Nanostructures. *Nature* **1995**, *375*, 564–567.
19. Schmidt, O. G.; Ebert, K. Nanotechnology—Thin Solid Films Roll up into Nanotubes. *Nature* **2001**, *410*, 168–168.
20. Sha, J.; Niu, J. J.; Ma, X. Y.; Xu, J.; Zhang, X. B.; Yang, Q.; Yang, D. R. Silicon Nanotubes. *Adv. Mater.* **2002**, *14*, 1219–1221.
21. Dai, Z. R.; Pan, Z. W.; Wang, Z. L. Gallium Oxide Nanoribbons and Nanosheets. *J. Phys. Chem. B* **2002**, *106*, 902–904.
22. Hirsch, P. B.; Howie, A.; Nicholson, R. B.; Pashley, D. W.; Whelan, M. J. *Electron Microscopy of Thin Crystals*; Butterworth: Washington, DC, 1965.
23. Buffat, P.; Borel, J. P. Size Effect on Melting Temperature of Gold Particles. *Phys. Rev. A* **1976**, *13*, 2287–2298.
24. Borel, J. P. Thermodynamical Size Effect and the Structure of Metallic Clusters. *Surf. Sci.* **1981**, *106*, 1–9.
25. Lide, D. R. *CRC Handbook of Chemistry and Physics*, 71st ed.; Chemical Rubber Co.: Cleveland, OH, 1990.
26. Hsu, W. K.; Terrones, M.; Terrones, H.; Grobert, N.; Kirkland, A. I.; Hare, J. P.; Prassides, K.; Townsend, P. D.; Kroto, H. W.; Walton, D. R. M. Electrochemical Formation of Novel Nanowires and Their Dynamic Effects. *Chem. Phys. Lett.* **1998**, *284*, 177–183.
27. Yokota, T.; Murayama, M.; Howe, J. M. In Situ Transmission-Electron-Microscopy Investigation of Melting in Submicron Al-Si Alloy Particles under Electron-Beam Irradiation. *Phys. Rev. Lett.* **2003**, *91*, 265504.
28. Yuan, D. W.; Yan, R. F.; Simkovich, G. Rapid Oxidation of Liquid Tin and Its Alloys at 600 to 800 Degrees C. *J. Mater. Sci.* **1999**, *34*, 2911–2920.
29. Hu, J. Q.; Ma, X. L.; Shang, N. G.; Xie, Z. Y.; Wong, N. B.; Lee, C. S.; Lee, S. T. Large-Scale Rapid Oxidation Synthesis of SnO_2 Nanoribbons. *J. Phys. Chem. B* **2002**, *106*, 3823.
30. Hu, J. Q.; Bando, Y.; Zhan, H. J.; Golberg, D. Sn-Filled Single-Crystalline Wurtzite-Type ZnS Nanotubes. *Angew. Chem., Int. Ed.* **2004**, *43*, 4606–4609.
31. Hu, J. Q.; Bando, Y.; Zhan, H. J.; Liu, Z. W.; Golberg, D.; Ringer, S. P. Single-Crystalline, Submicrometer-Sized ZnSe Tubes. *Adv. Mater.* **2005**, *17*, 975–979.
32. Hu, J. Q.; Bando, Y.; Zhan, H. J.; Liao, M. Y.; Golberg, D.; Yuan, X. L.; Sekiguchi, T. Single-Crystalline Nanotubes of IIB-VI Semiconductors. *Appl. Phys. Lett.* **2005**, *87*, 113107.
33. The source of oxygen that contributed to the formation of the β-Ga_2O_3 RSTs may have several origins. Most likely, oxygen may come from that adsorbed on a Si wafer due to air exposure during processing. Another possible source is the residual oxygen inside the vacuum system, as the base pressure (2×10^{-2} Torr) in it was relatively high. The inevitable leakage of the vacuum system may also be a source, as the synthesis is conducted in an alumina tube that is sealed by an O-ring (see the experimental apparatus in ref 12).
34. Dai, Z. R.; Pan, Z. W.; Wang, Z. L. Novel Nanostructures of Functional Oxides Synthesized by Thermal Evaporation. *Adv. Funct. Mater.* **2003**, *13*, 9–24.
35. Ding, Y.; Wang, Z. L. Structure Analysis of Nanowires and Nanobelts by Transmission Electron Microscopy. *J. Phys. Chem. B* **2004**, *108*, 12280–12291.
36. Pan, Z. W.; Dai, Z. R.; Ma, C.; Wang, Z. L. Molten Gallium as a Catalyst for the Large-Scale Growth of Highly Aligned Silica Nanowires. *J. Am. Chem. Soc.* **2001**, *124*, 1817–1822.
37. Hu, J. Q.; Jiang, Y.; Meng, X. M.; Lee, C.-S.; Lee, S.-T. Temperature-Dependent Growth of Germanium Oxide and Silicon Oxide Based Nanostructures, Aligned Silicon Oxide Nanowire Assemblies, and Silicon Oxide Microtubes. *Small* **2005**, *1*, 429–438.